Supporting Information

Self-Assembly of Water-Soluble Silver Nanoclusters: Superstructure Formation and Morphological Evolution

Jinglin Shen [a], Zhi Wang [a], Di Sun[a] *, Guokui Liu[a], Shiling Yuan [a] *, Mohamedally Kurmoo [c], Xia Xin [a, b] *

*Author to whom correspondence should be addressed, E-mail: xinx@sdu.edu.cn.

Phone: +86-531-88363597. Fax: +86-531-88361008

* Author to whom correspondence should be addressed, E-mail: shilingyuan@sdu.edu.cn.

Phone: +86-531-88365896. Fax: +86-531-88564750

*Author to whom correspondence should be addressed, E-mail: dsun@sdu.edu.cn

Phone: +86-531-88364218. Fax: +86-531-88364216

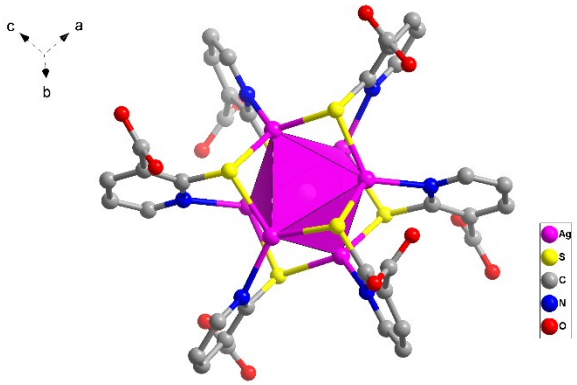

Figure S1. The molecular structure of $Ag_6(mna)_6^{6-}$.

Structure description of $\{(NH_4)_6[Ag_6(mna)_6]\cdot 9H_2O\}$,Ag_6-NC, and its solution behavior

X-ray single-crystal diffraction data of Ag_6-NC reveals that the hexanuclear cluster crystallized in triclinic space group *P*-1 and its asymmetric unit consists of a half of Ag_6-NC and 4.5 water molecules in the crystal lattice (Figure S1). In order to examine the solution stability of compound Ag_6-NC, we investigate the high-resolution electrospray mass spectrometry (HR-ESI-MS) of Ag_6-NC dissolved in water in the negative region (Figure S2). The HR-ESI-MS of Ag_6-NC displays two major signals centered at *m/z* = 1260.3918 (**1a**) and 1282.3745 (**1b**) in the range of 1000-2000. After careful analysis, these two monovalent charged peaks could be assigned to $[Ag_6(mna)_4H]^-$(calc. *m/z* = 1260.3904) and $[Ag_6(mna)_4Na]^-$(*calc*. *m/z* = 1282.3723), indicating that Ag_6-NC is stable in aqueous solution.

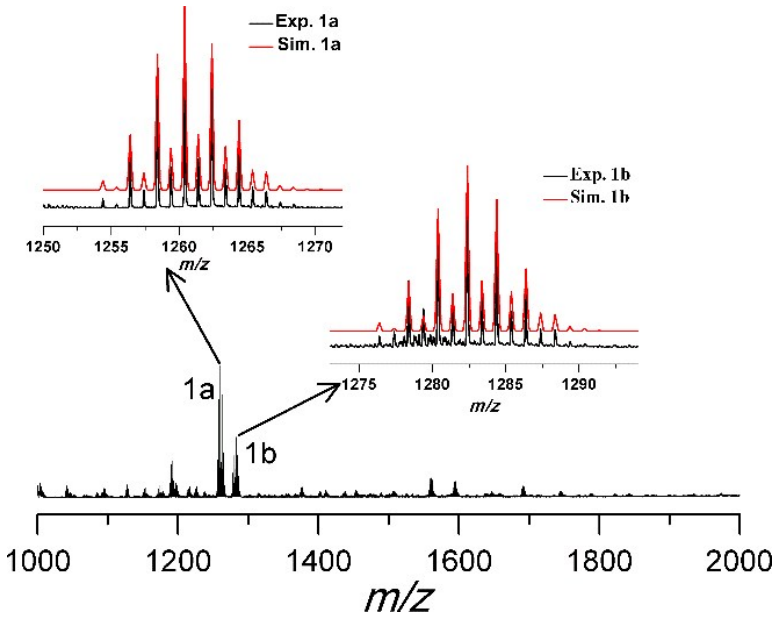

Figure S2. HR-ESI-MS in negative mode of Ag_6-NC dissolved in water. Insets: Enlarged portion of the spectra showing the experimental (black) and simulated (red) isotopic distribution patterns.

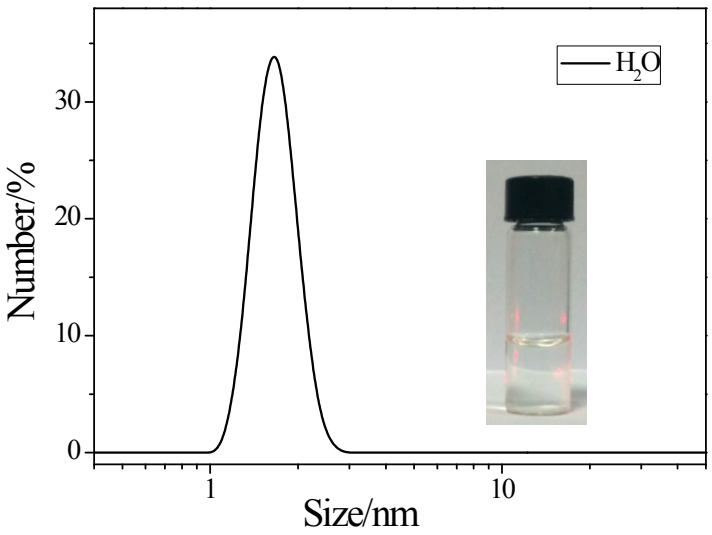

Figure S3. Dynamic laser scattering (DLS) result for Ag_6-NC in water at 100 μM and sample image under laser irradiation.

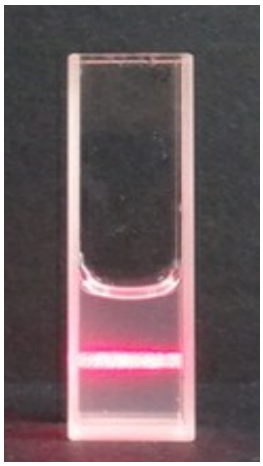

Figure S4. Tyndall phenomenon of Ag_6-NC in EG at 50 μM.

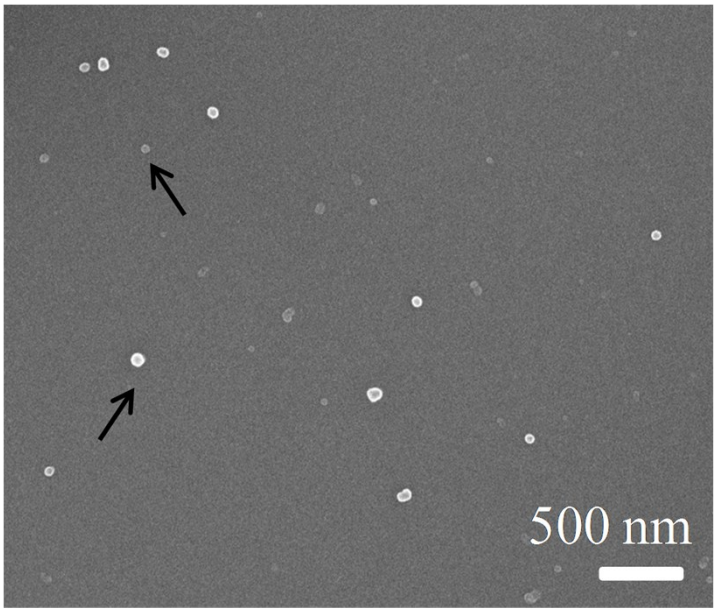

Figure S5. SEM images of the sample of Ag_6-NC in EG solvent (c = 50μM).

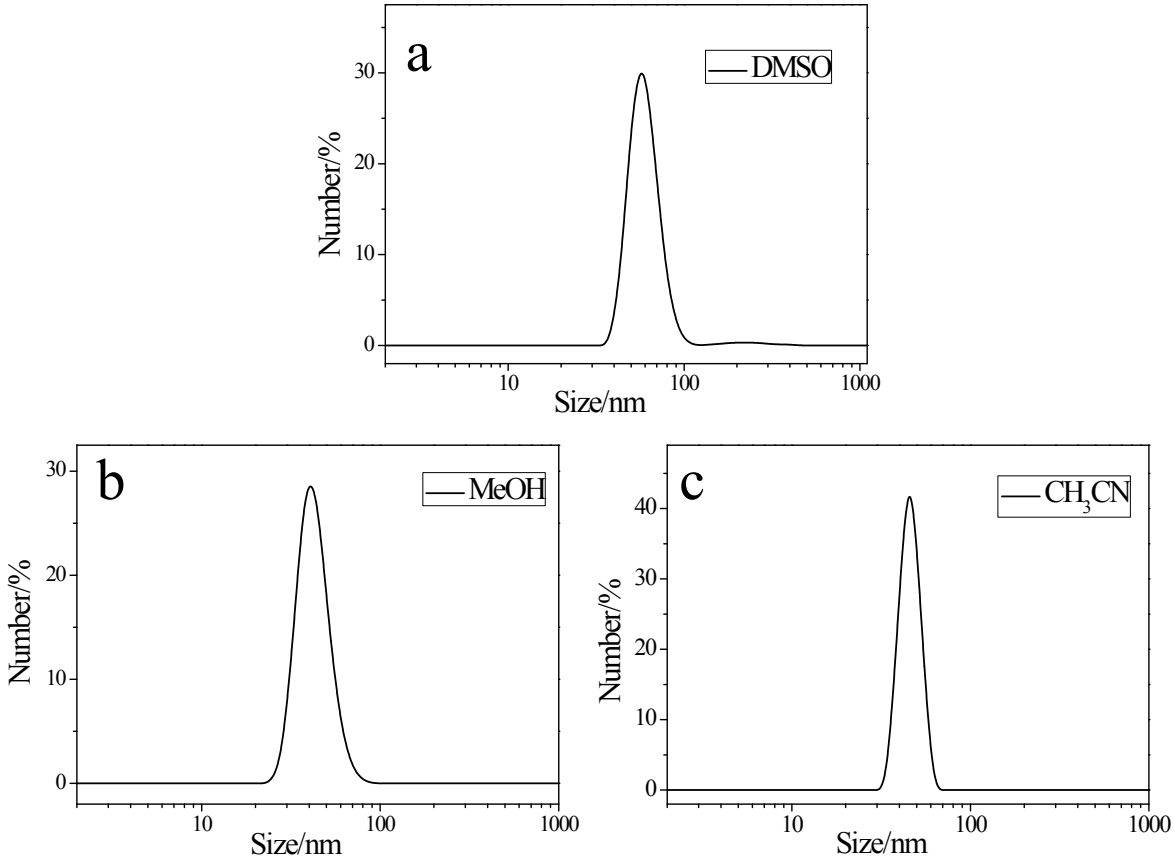

Figure S6. DLS results of Ag_6-NC in (a) DMSO, (b) MeOH and (c) CH_3CN.

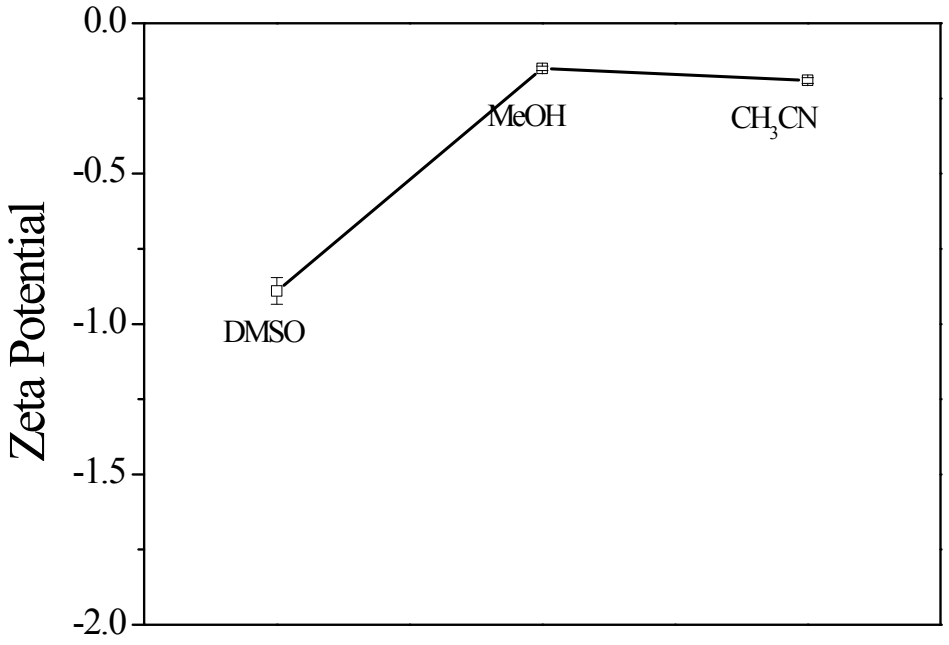

Figure S7. Zeta potential results of Ag_6-NC in (a) DMSO, (b) MeOH and (c) CH_3CN.

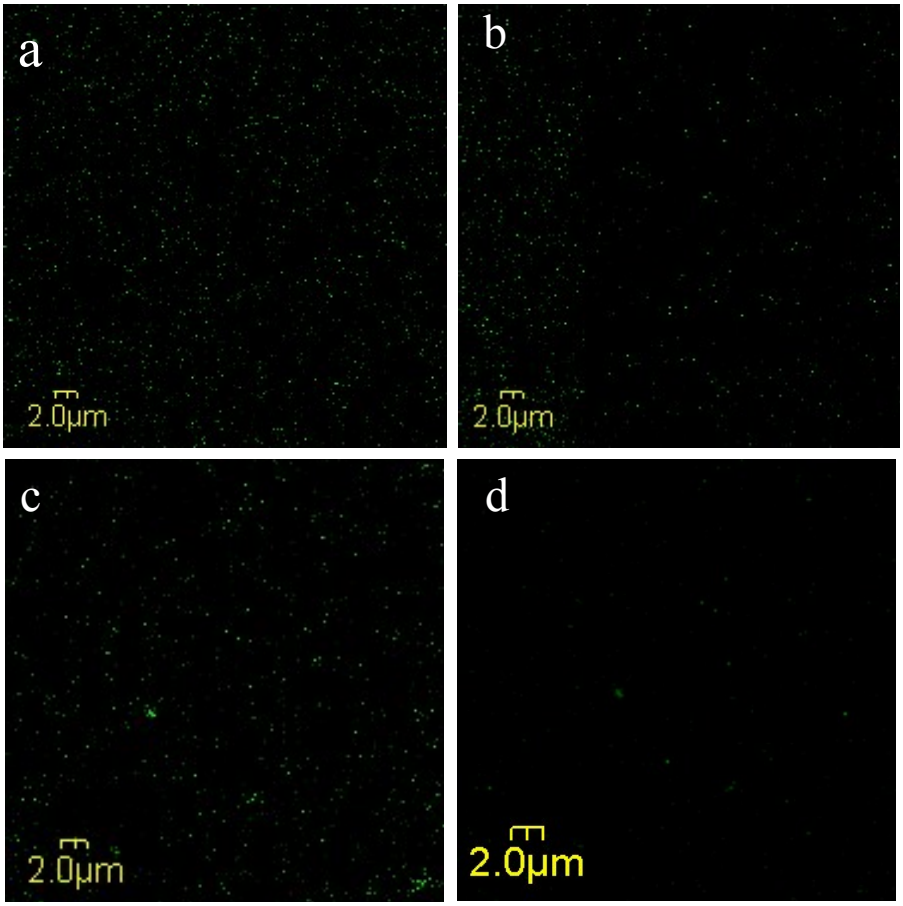

Figure S8.Confocal laser scan microscopy (CLSM) results of Ag_6-NC in (a) EG, (b) DMSO, (c) MeOH and (d) CH_3CN.

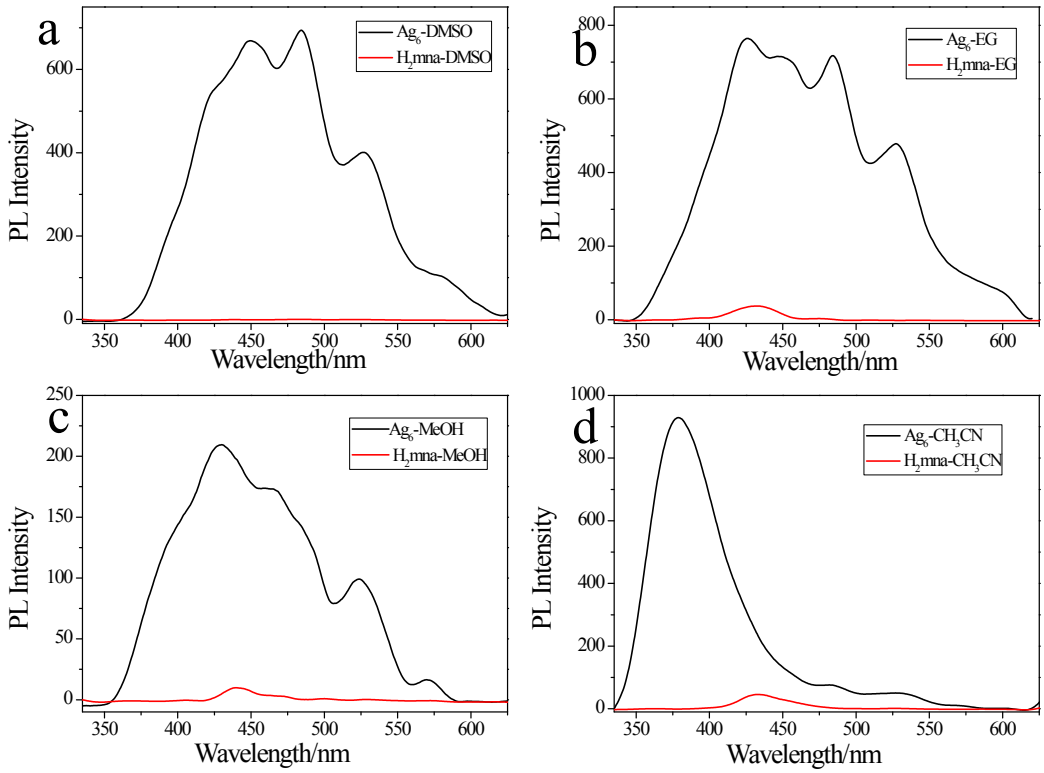

Figure S9. FL spectra of Ag_6-NC and free H_2mna in different solvents at the same concentration.

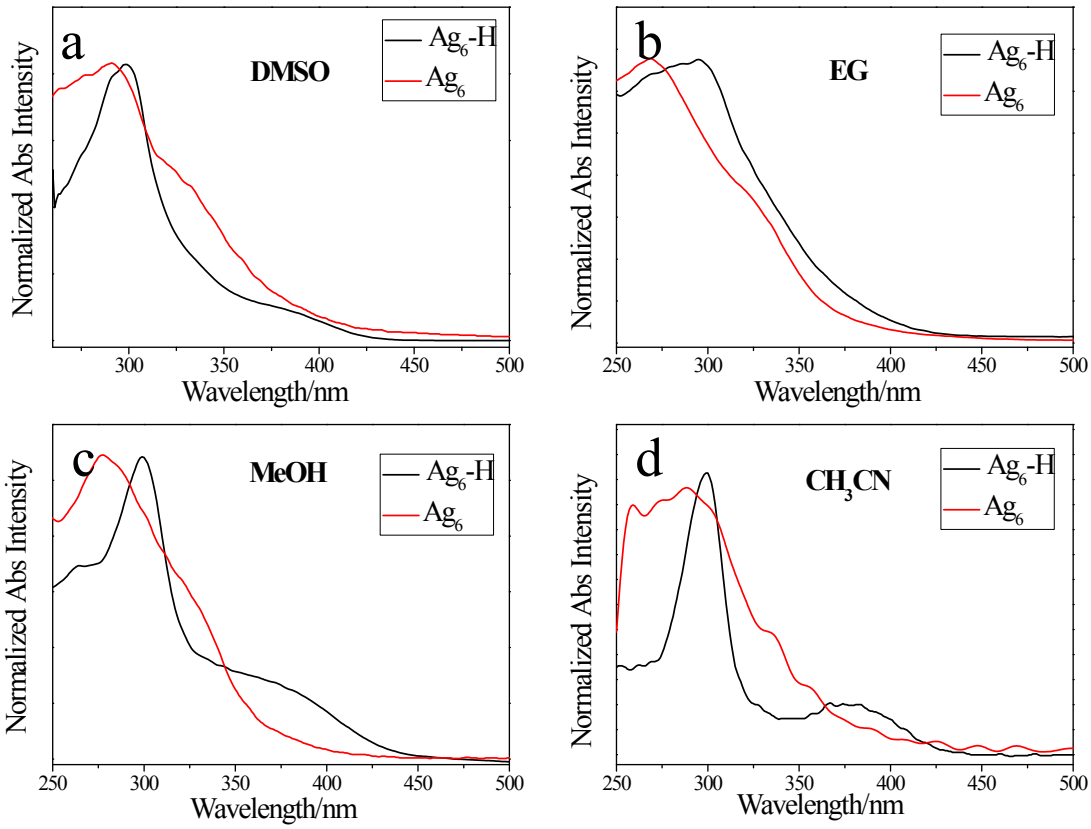

Figure S10. UV-vis spectra of Ag_6-NC and Ag_6-H-NC.

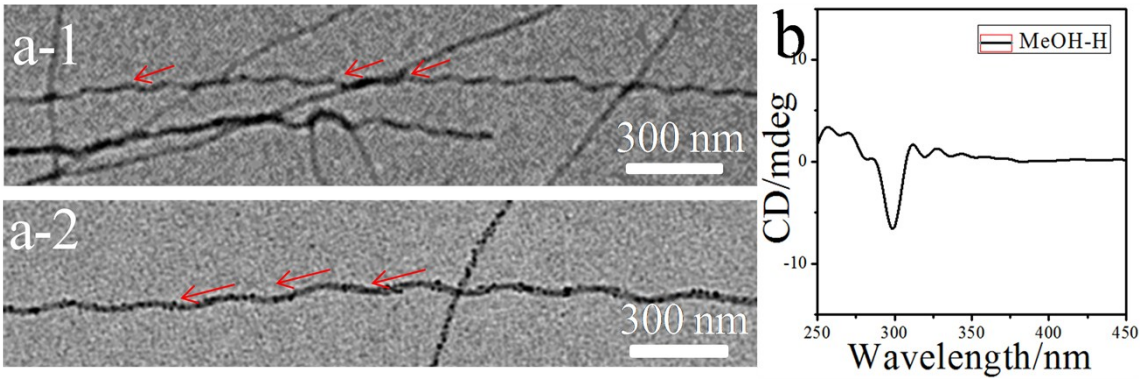

Figure S11. (a) TEM images and (b) CD spectra of Ag_6-H-NC in MeOH at *c*=20 μM.

The nanowires appear to twist in MeOH as shown in Figure S11 a. In circular dichroism (CD) spectra, an noticeable negative Cotton effect at 300 nm, suggesting that the formation of supramolecular chiral aggregates. (Figure S11 b) Helical morphology is a rather common and fascinating phenomenon in nature. Generally, helical structures are achieved by the controlled assembly of intrinsically chiral or achiral species in the presence of chiral constituents. Specially, completely achiral molecules with π-conjugation systems could also be capable self-assemble into helical nanostructures. The supramolecular chirality obtained from the self-assembly of achiral molecule Ag_6-H-**NC** is expected to be solvent-bridged hydrogen bonding interaction and the π-conjugation structure of Ag_6-H-NC. The reasons for this phenomenon are not very clear, and further studies will be made in the future.

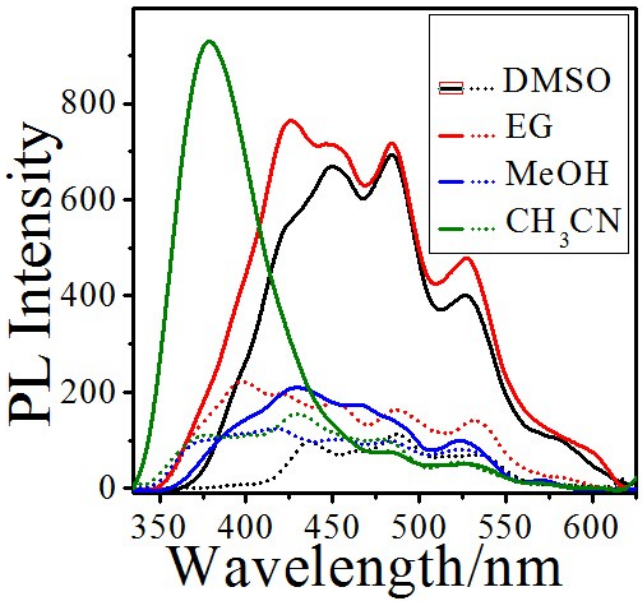

Figure S12. Fluorescence spectra of Ag_6-NC (solid line) and Ag_6-H-NC (dotted line) in different solvents with the same concentration.

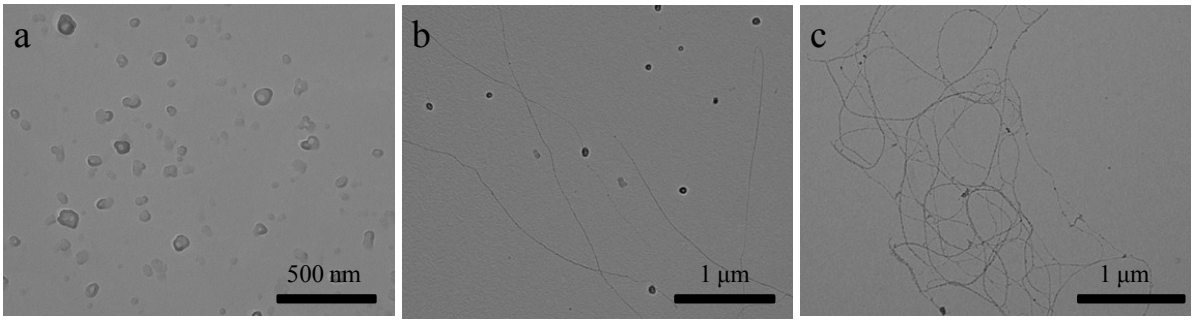

Figure S13.TEM images of Ag_6-H-NC in MeOH at different times. (a) 20 mins, (b) 10h (c) 1 day.(*c*=20 μM).

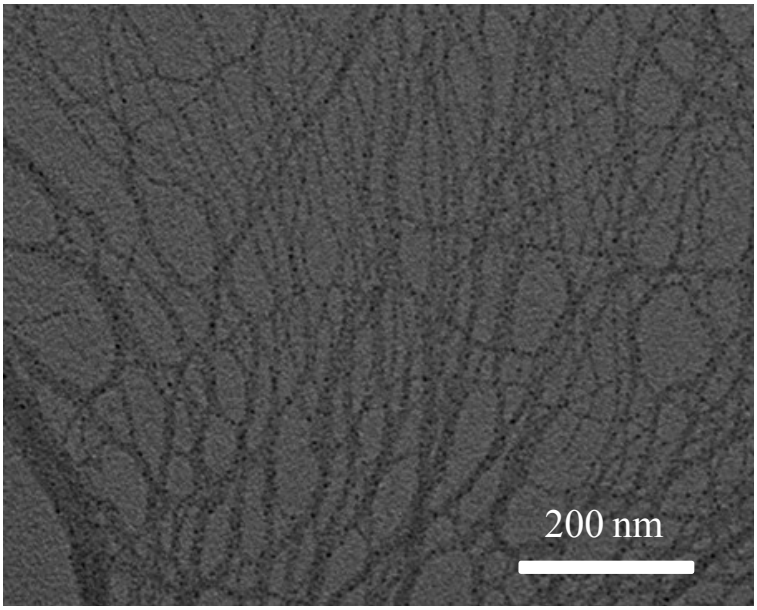

Figure S14. TEM image of Ag_6H-NC in water (c=50 μM).

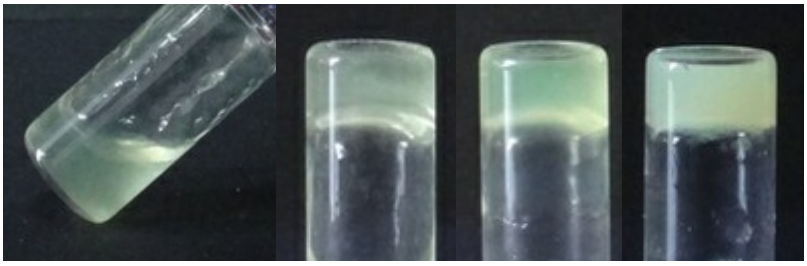

Figure S15. Phase behavior of Ag_6-H-**NC** at different concentrations. (From left to right:2 mM, 3 mM, 6 mM, 8 mM).

Figure S16. Phase behavior of H_2mna at c=48mM.

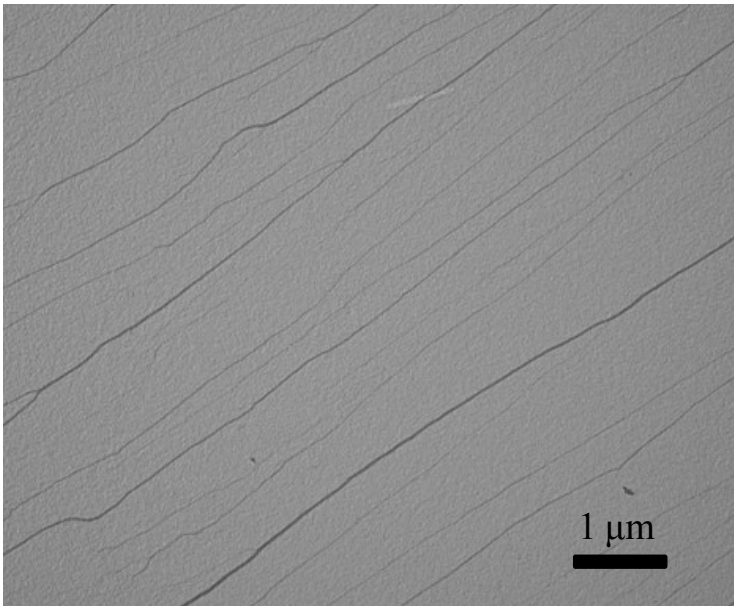

Figure S 17. TEM image of hydrogel (*c*=3 mM).

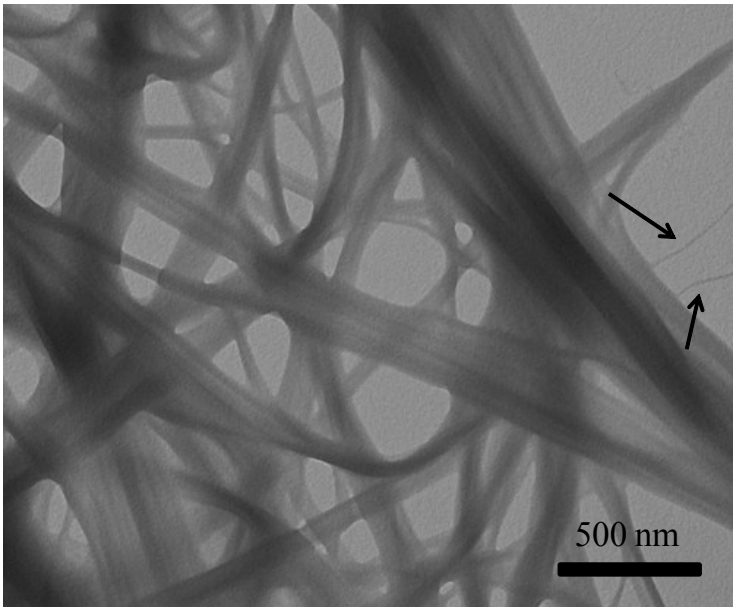

Figure S 18. TEM image of hydrogel (*c*=6 mM).

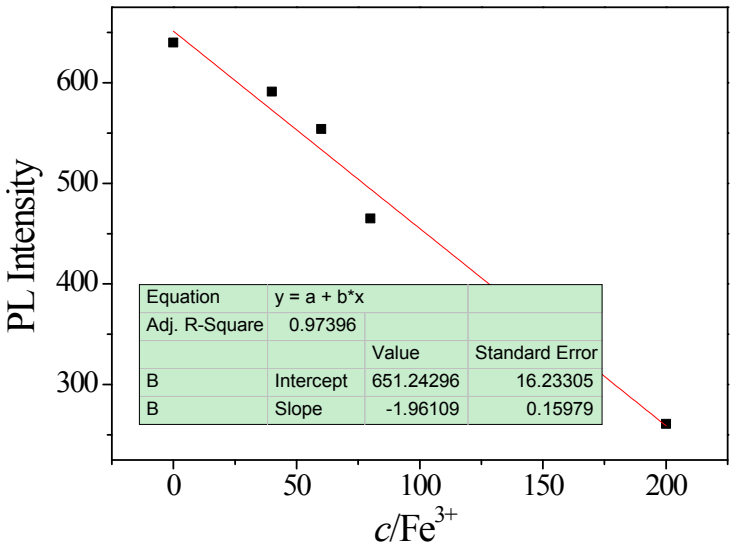

Figure S19. The linear relationship of I_{485} *vs*. concentration of Fe^{3+} in the range of 0–200 μM for 50 μM Ag_6-NC.

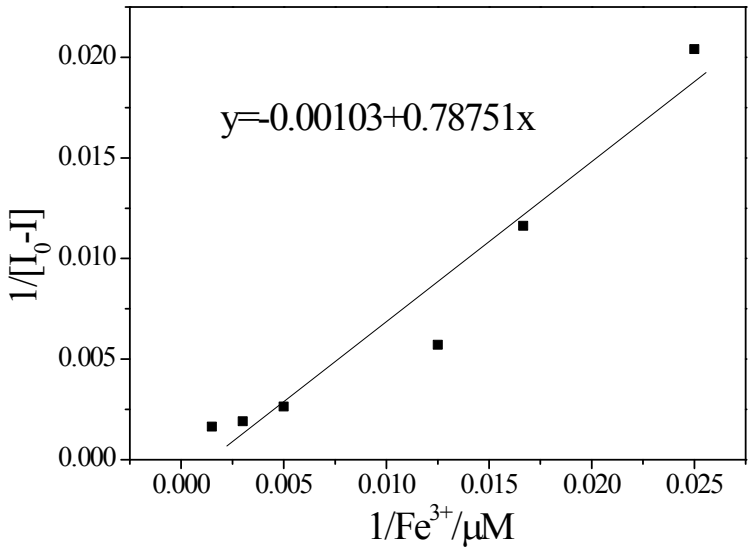

Figure S20. The linear relationship of $1/(I-I_0)$ vs.$1/Fe^{3++}$ for 50 μM Ag_6-NC.